ASTROBIOLOGY
Volume 9, Number 10, 2009
© Mary Ann Liebert, Inc.
DOI: 10.1089/ast.2008.0316

Phyllosilicate Emission from Protoplanetary Disks: Is the Indirect Detection of Extrasolar Water Possible?

Melissa A. Morris[1,2] and Steven J. Desch[1]

Abstract

Phyllosilicates are hydrous minerals formed by interaction between rock and liquid water, and are commonly found in meteorites that originate in the asteroid belt. Collisions between asteroids contribute to zodiacal dust, which therefore reasonably could include phyllosilicates. Collisions between planetesimals in protoplanetary disks may also produce dust that contains phyllosilicates. These minerals possess characteristic emission features in the mid-infrared and could be detectable in extrasolar protoplanetary disks. We have determined whether phyllosilicates in protoplanetary disks are detectable in the infrared, using instruments such as those on board the Spitzer Space Telescope and the Stratospheric Observatory for Infrared Astronomy (SOFIA). We calculated opacities for the phyllosilicates most common in meteorites and, using a two-layer radiative transfer model, computed the emission of radiation from a protoplanetary disk. We found that phyllosilicates present at the 3% level lead to observationally significant differences in disk spectra and should therefore be detectable with the use of infrared observations and spectral modeling. Detection of phyllosilicates in a protoplanetary disk would be diagnostic of liquid water in planetesimals in that disk and would demonstrate similarity to our own Solar System. We also discuss use of phyllosilicate emission to test the "water worlds" hypothesis, which proposes that liquid water in planetesimals should correlate with the inventory of short-lived radionuclides in planetary systems, especially ^{26}Al. Key Words: Water—Protoplanetary disks—Infrared emission—Phyllosilicates. Astrobiology 9, 965–978.

Introduction

Terrestrial planets and water

In the search for extraterrestrial life, it is extremely important to attempt to detect water in extrasolar planetary systems, particularly on terrestrial planets. The central requirements for life as we know it are a source of free energy, a source of carbon, and liquid water (Chyba *et al.*, 2000). Chyba *et al.* (2000) purported that "where there is liquid water, there is the possibility of life as we know it." So far, the detection of water on a terrestrial exoplanet has not been achieved, though there are hints that liquid water may occur on such planets. Close-in extrasolar giant planets (hot Jupiters) have been observed to have water vapor in their atmospheres (Beaulieu *et al.*, 2008), and water vapor emission from a protoplanetary disk was recently observed as well (Watson *et al.*, 2007; Carr and Najita, 2008). However, the search for liquid water on *Earth-like* planets is extremely difficult. Should an Earth-like planet be discovered, strategies exist for detecting liquid water on the surface (Williams and Gaidos, 2008). To date, no such planets have been found; the most Earth-like planet yet discovered is Gliese 581c (Selsis *et al.*, 2007; Udry *et al.*, 2007), which is nearly 5 times the mass of Earth.

Another approach to the search for liquid water on terrestrial planets is to follow the path upstream to the water's source. While not universally accepted, it is generally thought that the majority of Earth's water was delivered by planetesimals from the outer asteroid belt (Morbidelli *et al.*, 2000; Raymond *et al.*, 2004; Mottl *et al.*, 2007). We refer the reader to these papers, whose arguments we attempt to summarize here. Comets have long been suggested as a source of Earth's water (Owen and Bar-Nun, 1995), but the low terrestrial D/H ratio suggests otherwise (Drake and Righter, 2002). In fact, in the few comets for which the D/H ratio has been measured, it is twice that for Earth; the D/H ratio would not be reduced by chemical fractionation processes (Eberhardt *et al.*, 1995; Bockelee-Morvan *et al.*, 1998; Meier *et al.*, 1998). In addition, comets are predicted to introduce too much Ar and other noble gases to be consistent with the low terrestrial Ar/H_2O ratio (Owen and Bar-Nun,

---

[1] School of Earth and Space Exploration, Arizona State University, Tempe, Arizona.
[2] Present address: Department of Physics, Astronomy, and Materials Science, Missouri State University, Springfield, Missouri.

1995; Swindle and Kring, 1997; Morbidelli *et al.,* 2000). Finally, the likelihood of sufficient comets colliding with Earth is too low to account for Earth's volatile content (Morbidelli *et al.,* 2000; Levison *et al.,* 2001). Drake and Righter (2002) claimed that, during its formation, Earth received no more than 50% of its water from comets; based on dynamical arguments, Morbidelli *et al.* (2000) claimed the fraction is less than 10% of Earth's present water budget.

Both Drake and Righter (2002) and Morbidelli *et al.* (2000) instead strongly argued that the Earth accreted "wet," with asteroids or planetesimals from the outer asteroid belt as the main source of the water. The D/H ratio in Vienna standard mean ocean water is consistent with that of carbonaceous chondrites, both having D/H ratios of 150 ppm (Drake and Righter, 2002). As reviewed by Morbidelli *et al.* (2000), carbonaceous chondrites, which are associated spectrally with C-type asteroids (Gradie and Tedesco, 1982) and believed to have formed in the outer asteroid belt (*i.e.,* beyond 2.5 astronomical units), contain ~10 wt % water (structurally bound in clays), whereas ordinary and enstatite chondrites, which are associated spectrally with S- and E-type asteroids from the inner belt (Gradie and Tedesco, 1982), contain ~0.5–0.1 wt % water. Accretion of a few percent of Earth's mass from carbonaceous chondritic material from beyond 2.5 astronomical units (AU) is sufficient to explain Earth's volatile content (Morbidelli *et al.,* 2000; Mottl *et al.,* 2007). Complications to this hypothesis include the difference in oxygen isotopic content between Earth and carbonaceous chondrites and the abundances of siderophiles like Os carried by carbonaceous chondrites (Drake and Righter, 2002). However, reasonable refutations to these objections exist (Mottl *et al.,* 2007). Accordingly, we have assumed that Earth and extrasolar terrestrial planets acquired their water during accretion, from planetesimals. If this is the case, then the volatile content of the planetesimals themselves largely governs how much water or other volatiles a planet will eventually possess. Of course, volatiles may be lost during impacts, and the fraction of water sequestered in the mantle versus that which is outgassed to the surface is not known. All other things being equal, if the planetesimals that make up a terrestrial planet have twice the amount of water than the planetesimals that made up Earth, it may reasonably be expected that such a planet would have twice as much water in its oceans than does Earth.

Planetesimal volatiles and ^{26}Al

Desch and Leshin (2004) pointed out that, if the volatile content of terrestrial planets is determined by the volatile content of the planetesimals from which they formed, then ultimately it will depend on the abundance of ^{26}Al in the planetary system. A general consensus is that the internal heating of asteroids in the Solar System was due to the presence of radioactive ^{26}Al ($t_{1/2} = 0.7$ Myr) in these bodies (Grimm and McSween, 1993; Lugmair and Shukolyukov, 2001; Huss *et al.,* 2001; McSween *et al.,* 2002; Gilmour and Middleton, 2009). Grimm and McSween (1993) explained the heliocentric zoning of the asteroid belt based on this heat source. At the time of the formation of calcium-rich, aluminum-rich inclusions (CAIs), the ^{26}Al abundance in the Solar System was $^{26}\text{Al}/^{27}\text{Al} = 5\times10^{-5}$ (MacPherson *et al.,* 1995). Asteroids that reached sizes that led to the trapping of radiogenic heat (roughly 30 km in diameter) in the first 2.6 Myr after CAIs formed would thus have incorporated enough live ^{26}Al ($^{26}\text{Al}/^{27}\text{Al} > 4\times10^{-6}$) to differentiate completely, as was likely the case for Vesta. Asteroids that grew this large from 2.6–4.5 Myr after the formation of CAIs at the beginning of the Solar System would have incorporated less ($4\times10^{-6} > {}^{26}\text{Al}/^{27}\text{Al} > 5\times10^{-7}$) live ^{26}Al, enough to melt water ice but not rock. Such asteroids would be abundant in products of aqueous alteration, in particular, phyllosilicates. If peak temperatures in the asteroid exceeded 400°C, these phyllosilicates would have decomposed and devolatilized. Such asteroids would resemble S-type asteroids, the presumed parent bodies of ordinary chondrites. If peak temperatures did not exceed 400°C, asteroids within which water ice melted would have retained phyllosilicates and would resemble C-type asteroids, the presumed parent bodies of carbonaceous chondrites. Support for heating as the cause of devolatilization comes from the observed dichotomy inherent in the van Schmus-Wood classification scheme of chondrites; that they either retained abundant hydrated phases (petrologic types 1 and 2) *or* were heated above 400°C (petrologic types 3–6) (van Schmus and Wood, 1967; Weisberg *et al.,* 2006). Petrologic evidence from CV chondrites strongly indicates they devolatilized by heating (Krot *et al.,* 1995; Kojima and Tomeoka, 1996). In asteroids that incorporated even less live ^{26}Al ($^{26}\text{Al}/^{27}\text{Al} < 5\times10^{-7}$), ice would never have melted, and phyllosilicates would not have been produced. These asteroids presumably would resemble the D- and P-type asteroids of the outer asteroid belt. Radiogenic heating by ^{26}Al is a major control on planetesimal volatile inventory (Grimm and McSween, 1993; see also Gilmour and Middleton, 2009).

Grimm and McSween (1993) argued that the heliocentric zoning of the asteroid belt is a result of varying amounts of incorporated live ^{26}Al, due to increasing accretion times with increasing distance from the Sun. Asteroids inside 2.7 AU grew quickly enough (<2.6 Myr) to retain sufficient ^{26}Al to climb above 400°C, and now resemble the S-type asteroids. From 2.7 to 3.4 AU, less ^{26}Al was retained, the asteroids did not devolatilize, and C-type asteroids were produced. Beyond 3.4 AU, so little live ^{26}Al was incorporated by the time these planetesimals grew large, that ice in these bodies never melted, which resulted in D- and P-type asteroids. These zones are quite narrow and are not dependent on the amount of radiation received from the Sun (the internal temperatures of asteroids due to ^{26}Al decay, >700 K, are little affected by the Sun's luminosity).

Phyllosilicates apparently are produced on asteroids with just enough ^{26}Al to melt ice but not so much ^{26}Al that the asteroids devolatilize: $5\times10^{-7} < {}^{26}\text{Al}/^{27}\text{Al} < 4\times10^{-6}$. In our Solar System, this constraint implies that the ^{26}Al in CAIs decayed for 3–5 Myr from its initial value of $^{26}\text{Al}/^{27}\text{Al} = 5\times10^{-5}$. It is highly likely that this initial abundance of ^{26}Al was fixed by the amount of material the Solar System incorporated from a nearby supernova (Lee *et al.,* 1976; Hester *et al.,* 2004; Jacobsen, 2005; Wadhwa *et al.,* 2007), either from ejecta that contaminated its molecular cloud core (Cameron and Truran, 1977; Boss and Vanhala, 2000) or from ejecta injected into its already formed protoplanetary disk (Ouellette *et al.,* 2005, 2007; see also Looney *et al.,* 2006). Either way, injection of supernova material into a forming planetary system is a highly stochastic process, and other planetary systems are likely to have very different initial ^{26}Al abundances. Specifically, protoplanetary disks in regions that lack a massive star (*e.g.,* the Taurus-Auriga region) will incorporate no ^{26}Al from a nearby supernova and almost certainly have ^{26}Al/^{27}Al ratios orders of magnitude lower than was the case in our Solar System.

In a system with $^{26}\mathrm{Al}/^{27}\mathrm{Al} < 5\times10^{-7}$, ice would not melt on any planetesimals. Any planetesimals that formed in a part of a protoplanetary disk where ice condensed would contain abundant water ice and resemble D- and P-type asteroids. (The disk temperatures in a typical disk will not exceed the sublimation temperature of ice, 180 K, outside of about 0.7 AU (Chiang and Goldreich, 1997.) In such systems, no phyllosilicates would be produced on any planetesimals. On the other hand, terrestrial planets that form in such systems, mostly from planetesimals inside 2.6 AU (Raymond *et al.,* 2004, 2006), are likely to contain substantially more water than Earth, perhaps closer to tens of percent by weight. Planets in such ^{26}Al-poor systems would be "water worlds," the internal structures of which were explored by Léger *et al.* (2004). ^{26}Al-rich systems, like our Solar System, would possess planetesimals where ice melted and phyllosilicates were produced. Terrestrial planets in such systems are predicted to be "dry," like Earth. Likely regions to search for phyllosilicate emission from such systems would be protoplanetary disks in the Orion Ic and Id subgroups, whose O and Si abundances strongly suggest contamination by supernovae in the Orion Ia and Ib subgroups (Cunha and Lambert, 1992, 1994; Cunha *et al.,* 1998).

The hypothesis that planetesimals in star-forming regions like Taurus will be ice-rich and result in water-rich terrestrial planets, or "water worlds," admittedly is based on a number of assumptions. One prediction of this water worlds hypothesis that can be tested is the expectation that the dust in protoplanetary disks in regions like Taurus-Auriga will not exhibit phyllosilicates. We predict that phyllosilicates are possible only in systems that formed near a supernova, with abundant ^{26}Al. If the material in ^{26}Al-rich, phyllosilicate-bearing planetesimals is returned to the protoplanetary disk, and if phyllosilicates can be spectrally distinguished, then phyllosilicate emission is predicted to be found in these ^{26}Al-rich systems, and in these systems only.

Mid-infrared (MIR) spectra

Strong observational evidence for disks around young stellar objects (YSOs) and T Tauri stars exists, especially in the form of excess infrared emission over what would be expected from the stellar photosphere alone (Adams *et al.,* 1988; McCaughrean and O'Dell, 1996; Chiang and Goldreich, 1997; de Pater and Lissauer, 2001). In fact, IR excess emission is observed in 25–50% of pre-main-sequence stars of 1 solar mass ($M_\odot$) (de Pater and Lissauer, 2001). The excess IR emission is the result of thermal emission due to reprocessed starlight from circumstellar dust grains (Adams *et al.,* 1988; Hartmann, 1998). During the T Tauri stage, the system consists of a passive, reprocessing disk, in which the excess infrared emission originates from dust grains in the outer layers of the disk that are heated by starlight (Kenyon and Hartmann, 1987).

The spectra of YSOs with IR excesses contain information about the composition of the dust that gives rise to that emission. While observations at millimeter wavelengths probe closer to the midplane of the disk, MIR observations probe the surface layers of the disk. The spectra of YSOs routinely exhibit silicate emission bands at $\lambda \sim 10\,\mu$m and $\lambda \sim 20\,\mu$m. This implies that the grains are emitting in the Rayleigh limit, $a \geq \lambda/2\pi$, where a is the radius of the grain, as the observed silicate feature should diminish if the particle was more than a few microns in size (Pollack *et al.,* 1994; Nakamura, 1998). The silicate band positions and profiles are highly diagnostic of stoichiometry (Dorschner *et al.,* 1995; Fabian *et al.,* 2001; Krishna Swamy, 2005). Phyllosilicates exhibit the 10 and 20 μm features characteristic of silicates, with distinctive substructure particular to each specific mineral (Fig. 1). All phyllosilicates also show a distinct absorption feature at 6 μm and other wavelengths due to structural H_2O. The unique and distinctive MIR spectral features of silicates in general and phyllosilicates in particular make the study of the mineralogy of protoplanetary disks possible.

The disk environment

Forming planetary systems are generally observed in one of two states: the protoplanetary disk stage, when gas and dust are both present and presumed similar in properties to interstellar material; and the debris disk stage, after gas has been removed and only dust from collisions between planetesimals is present. Examples of protoplanetary disks are abundant (Adams *et al.,* 1987) and include the archetype T Tauri. The fraction of disks in a cluster observed to possess protoplanetary disks tends to decrease with age of the cluster, dropping below 50% at 3–6 Myr (Haisch *et al.,* 2001). Examples of debris disks include β Pic (Smith and Terrile, 1984) and AU Mic (Kalas *et al.,* 2004), both of which are members of the 12 Myr old β Pic moving group (Zuckerman *et al.,* 2001). Objects apparently in transition between the two also exist, such as TW Hya (Calvet *et al.,* 2002). Since the formation of terrestrial planets takes several tens of Myr (Wadhwa and Russell, 2000), debris disks would, ideally, be better to observe, as they would contain only dust from planetesimals at the time terrestrial planets are forming. Unfortunately, debris disks are too faint to search for the infrared signatures of phyllosilicates. The average column density of debris disks ranges from $\sim 10^{-4}$ to $\sim 10^{-7}$ g cm^{-2}, as compared to the column density in the superheated dust layer of a protoplanetary disk, which is on the order of $\sim 10^{-2}$ g cm^{-2} (Chiang and Goldreich, 1997). The dust emission features (which can arise only in the optically thin portions of disks) are therefore several orders of magnitude weaker in debris disks than in protoplanetary disks. The fluxes from the nearest debris disk, β Pictoris, are sufficiently large to detect the dominant emission features, such as crystalline and amorphous silicates (Okamoto *et al.,* 2004); but, as we show below, the fluxes in debris disks are too low to detect features that are a few percent on the continuum, such as the phyllosilicates we consider here. We therefore do not consider debris disks further and turn our attention to protoplanetary disks.

If protoplanetary disks contain predominantly interstellar dust, then their spectra would not yield any new information

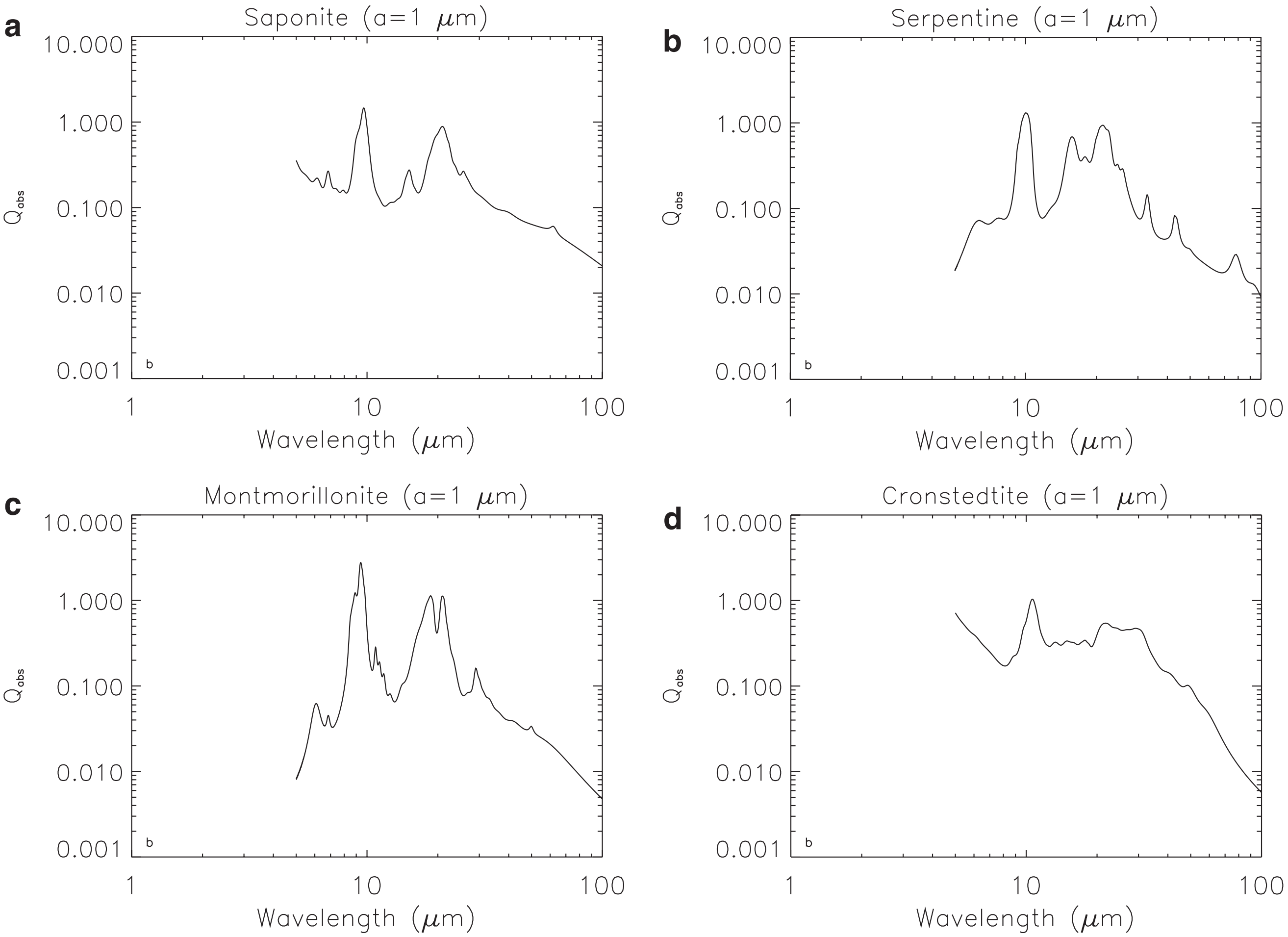

FIG. 1. The absorption efficiency factor, Q_{abs}, for (**a**) saponite, (**b**) serpentine, (**c**) montmorillonite, and (**d**) cronstedtite calculated from *n* and *k* determined by Glotch *et al.* (2007).

about the processes in the disk or the composition of planetesimals in them. Protoplanetary disks do not, however, contain pure interstellar dust. The existence of crystalline silicates argues strongly for thermal processing of dust within them (*e.g.*, Wooden *et al.*, 2007), as the interstellar medium contains only (>99.8%) amorphous silicates (Kemper *et al.*, 2004). Dust samples from comet 81P/Wild 2, which were returned as a part of the STARDUST mission, have been shown to have a solar isotopic composition (Brownlee *et al.*, 2006; Stephan, 2008; Zolensky *et al.*, 2008), which indicates processing in the early Solar System. Observations of Orion proplyds also indicate growth of the minimum grain size in the first few $\times 10^5$ years (Throop *et al.*, 2001). This is *not* interpreted to mean that grains took $>10^5$ years to collide. Quite the contrary, micron-sized grains coagulate and fragment on timescales <10 years, typically, and thus a quasi–steady-state grain size distribution is rapidly established; it is the mean size of the distribution that evolves over long time periods (Throop *et al.*, 2001).

Numerical models also predict rapid grain growth, from submicron size to planetesimals tens of kilometers in diameter: $<10^4$ yr at 3 AU (Woolum and Cassen, 1999; Weidenschilling, 2000; Weidenschilling and Cuzzi, 2006). In fact, the basaltic howardite, eucrite, and diogenite achondrites [spectrally associated with the 200 km diameter asteroid, 4 Vesta: Drake (1979)] formed on a fully differentiated body. Al-Mg isotopic studies have shown that their parent body differentiated *and crystallized* within, at most, 5 Myr after the formation of the first solids in the Solar System, CAIs (Srinivasan *et al.*, 1999). Bodies tens of kilometers in diameter that formed within the first 4 Myr of our Solar System contained sufficient ^{26}Al to melt water ice within them (Grimm and McSween, 1993), which would have potentially led to phyllosilicate production on these bodies by processes such as serpentinization (Cohen and Coker, 2000). If similarly sized bodies are also forming in protoplanetary disks, and if these bodies are also collisionally ground to dust during this stage, much of the dust seen in protoplanetary disks could be a mix of interstellar dust that has coagulated and been processed in the nebula, plus dust shed by planetesimals, akin to zodiacal dust.

Numerical simulations of the coagulation of dust and accretion of larger bodies, as well as the collisional disruption of bodies, strongly suggest that, at a few AU, planetesimals are built up and torn down on timescales <1 Myr (Weidenschilling, 2000). At any one time, about half the mass of solids at a few AU will reside in (roughly micron-sized) dust grains, with the other half residing in larger planetesimals

(Weidenschilling *et al.,* 1997; Weidenschilling 2000; Dullemond and Dominik, 2005; Brauer *et al.,* 2008; Johansen *et al.,* 2008). The dust is submicron in size because that is the size distribution that arises from a balance between coagulation and fragmentation. Intriguingly, this size distribution matches the sizes of matrix grains in chondrites (Brearley, 1996). This dust is *not* interstellar dust that simply has not yet had time to accrete into planetesimals. Rather, accretion models would indicate that it is primarily dust eroded from the larger planetesimals in the disk.

A simple analysis of asteroidal erosion also yields the same conclusion, that dust is primarily derived from larger bodies. In the current Solar System, there is approximately 10^{20} g of zodiacal dust shed from asteroids (Nesvorny *et al.,* 2006) or the sublimation of comets (Lisse, 2002). Assuming a typical grain radius of 10 microns, these dust grains have a lifetime against Poynting-Robertson drag $\cong 0.5$ Myr (Wyatt and Whipple, 1950), which implies a production rate of up to 2×10^{14} g yr^{-1}, due to asteroid-asteroid collisions. It is understood that the present-day asteroid belt is highly depleted relative to the primordial asteroid belt, by a factor of about 10^3 (Weidenschilling, 1977; Bottke *et al.,* 2005). If the primordial asteroid belt contained 1000 times the number of asteroids as it does today, and assuming the same velocity dispersions, the production rate of dust (proportional to the number density squared) would have been 2×10^{20} g yr^{-1}. Pumping of asteroid eccentricities by a primordial Jupiter (Weidenschilling *et al.,* 2001) could have increased the collision rate and the production rate even more. Collisions between planetesimals in protoplanetary disks should generate annually as much dust as is present in the Solar System zodiacal dust.

Unlike dust in a debris disk, dust in a protoplanetary disk is constrained to follow the gas and will not be lost to Poynting-Robertson drag. After 10^6 yr of collisions between asteroids, one might reasonably expect roughly 2×10^{26} g of dust to be shed from a primordial asteroid belt. This is to be compared to our assumed mass of the primordial asteroid belt itself, 1000 times the current mass of 3×10^{24} g, or about 3×10^{27} g (Bottke *et al.,* 2005). That is, something on the order of 7% of the nebular dust that grows to planetesimal size could be returned to the nebula gas as zodiacal dust on Myr timescales. This mass in asteroids roughly equaled the mass in dust at the same time; for the innermost few AU of a protoplanetary disk at least a few $\times10^5$ yr old, then, it is reasonable to conclude that a significant fraction, $\approx$7%, of the dust is eroded from planetesimals already formed in the disk.

If planetesimals in a protoplanetary disk have had time to grow and retain radioactive heat sufficient to melt water ice, the dust eroded from them could contain products of aqueous alteration. These products include carbonates and especially phyllosilicates (Mottl *et al.,* 2007). We focus on phyllosilicates because they are the most common products of aqueous alteration found in carbonaceous chondrites and interplanetary dust particles. The zodiacal dust in our own Solar System, derived from comets and asteroidal collisions, has a spectrum consistent with the inclusion of 20% abundance of the phyllosilicate montmorillonite (Reach *et al.,* 2003). As discussed below, phyllosilicates can comprise a large fraction of the mass in carbonaceous chondrites (40–90%). Assuming a mass fraction on the order of 50%, we expect that 3% of the dust in the nebula could be composed of phyllosilicates, especially in the regions (2–4 AU) that correspond to the location of the Solar System's asteroid belt. These phyllosilicates should radiate most strongly at $\sim$20 microns.

Phyllosilicates

Phyllosilicates are the major mineral product of aqueous alteration of silicate rock and therefore are excellent tracers of liquid water. Aqueous alteration on the parent body is believed to account for the majority of the phyllosilicates found in meteorites (Krot *et al.,* 2006), though fine-grained rims around chondrules may have been produced in the gas phase (Ciesla *et al.,* 2003). The water contained in carbonaceous chondrites is mainly in the form of these hydrous minerals. In the subclass of CI carbonaceous chondrites, anywhere from 40% to over 90% of the volume is made up of fine-grained phyllosilicates and associated phases (Tomeoka and Buseck, 1990; Buseck and Hua, 1993; Rubin, 1997). Phyllosilicates are also often found in the fine-grained rims around chondrules (Ciesla *et al.,* 2003, and references therein).

Virtually all carbonaceous chondrites contain phyllosilicates, with the different amounts indicating varying degrees of aqueous alteration. The subclasses that have experienced the most alteration are the CI, CM, and CR chondrites (Buseck and Hua, 1993; Rubin, 1997), which are significantly more altered than the CO and CV chondrites. The most common phyllosilicates found in meteorites (Table 1) are overwhelmingly saponite ($[\mathrm{Ca}/2,\mathrm{Na}]_{0.33}[\mathrm{Mg},\mathrm{Fe}^{2+}]_3[\mathrm{Si},\mathrm{Al}]_4\mathrm{O}_{10}[\mathrm{OH}]_2\cdot4\mathrm{H}_2\mathrm{O}$) and serpentine ($[\mathrm{Mg},\mathrm{Fe}]_3\mathrm{Si}_2\mathrm{O}_5[\mathrm{OH}]_4$), with montmorillonite ($[\mathrm{Na},\mathrm{Ca}]_{0.33}[\mathrm{Al},\mathrm{Mg}]_2\mathrm{Si}_4\mathrm{O}_{10}[\mathrm{OH}]_2\cdot n[\mathrm{H}_2\mathrm{O}]$) identified in the matrix of some CI chondrites and in the fine-grained rims of chondrules (Buseck and Hua, 1993). Cronstedtite ($\mathrm{Fe}_2^{2+}\mathrm{Fe}^{3+}[\mathrm{Si},\mathrm{Fe}^{3+}]\mathrm{O}_5[\mathrm{OH}]_4$), an Fe-rich phyllosilicate (Buseck and Hua, 1993; Lauretta *et al.,* 2000) rarely found terrestrially, makes up the bulk of the matrix of CM chondrites, along with intergrowths of serpentine (Buseck and Hua, 1993).

Outline

This paper is organized as follows. We first review the minerals expected in the "zodiacal dust" in protoplanetary disks, that is, those found in meteorites. We then discuss use of Mie theory to convert the complex index of refraction measured for these minerals into opacities. We then use a simple two-layer radiative transfer model to predict the spectral energy distributions (SEDs) from protoplanetary disks of varying mineralogies. We present our model SEDs with and without the inclusion of 3% phyllosilicates and

TABLE 1. PHYLLOSILICATES FOUND IN METEORITES

Saponite	*Serpentine*	*Montmorillonite*	*Cronstedtite*
CI	CM	CI	CM
CV	CO		
CR	CR		
Ordinary chondrites			
Interplanetary dust particles			

Table 2. Dust Composition in the Outer Disk

Species	*Mg*	*Fe*	*Si*	*S*	*C*
Olivine-type	0.83	0.42	0.63		
Pyroxene-type	0.17	0.09	0.27		
Quartz-type			0.10		
Iron		0.10			
Troilite		0.39		0.75	
Kerogen					0.55

From the model of Gail (2003, 2004).

show that the differences in the spectra are observable with many infrared instruments. We conclude that phyllosilicates are detectable by their infrared emission in protoplanetary disks. Finally, we discuss use of phyllosilicate emission to test the water worlds hypothesis that suggests that the water content of planetesimals and terrestrial exoplanets is linked to the abundance of short-lived radionuclides such as ^{26}Al (Desch and Leshin, 2004).

Methods

Minerals expected

The dust in protoplanetary disks is expected to consist primarily of compounds of the rock-forming elements (Si, O, Fe, Mg, Al, Ca, Na, S, Ni), along with carbonaceous compounds. Based on cosmic element abundances, the most abundant species should be compounds of Si, O, Mg, and Fe, plus carbon dust (Gail, 2003). Silicates are expected to be an amorphous non-equilibrium mixture in the outer portion of the disk, progressing through a crystalline non-equilibrium mixture in the middle portion of the disk, to a crystalline equilibrium mixture in the inner portion of the disk (Gail, 2003). Gail (2003, 2004) used the grain model of Pollack *et al.* (1994) to arrive at an outer disk composition of amorphous olivine, pyroxene, and quartz, solid iron and troilite, and kerogen. Kerogen was chosen as representative of the carbon-rich component of Pollack *et al.* (1994), as it is the carbonaceous material found in the matrix of carbonaceous chondrites (Gail, 2003). The relative abundances of these species are shown in Table 2. Gail (1998, 2003, 2004) estimated that the dust grains of the inner regions of the disk consist of pure, crystalline forsterite (Mg_2SiO_4) and enstatite ($MgSiO_3$), with the innermost regions iron-free and carbon-free, yet containing an aluminum component.

Based on the minerals expected in disks, the minerals considered in this study included both amorphous and crystalline olivines and pyroxenes (forsterite and enstatite), troilite (FeS), quartz (SiO_2), hibonite ($CaAl_{12}O_{19}$), and the phyllosilicates most commonly found in meteorites: saponite, serpentine, and montmorillonite. This list is hardly exhaustive and does not include amorphous carbon or other sources of continuum opacity. Inclusion of such minerals would be important if one were fitting an observed SED. Our purpose was to compare differences in computed spectra with and without phyllosilicates, so neglect of these other, relatively featureless minerals should not alter our conclusions.

Optical properties

To model and interpret the SEDs of protoplanetary disks, it is necessary to understand how the small dust particles in the surface layers of the disk interact with the radiation received from the central star. We consider the case in which the particles are small compared to the wavelength of radiation (within the Rayleigh limit). This is the appropriate limit needed for the production of observable MIR silicate features (Pollack *et al.*, 1994; Nakamura, 1998).

Dust particles in an accretionary disk of a YSO will result in the extinction of radiation emitted by the protostar by absorption and scattering. Extinction strongly depends on the size, shape, and chemical composition of the particles (Bohren and Huffman, 1983; Min *et al.*, 2003). The scattering and absorption properties of homogeneous spherical particles can be determined extremely accurately by utilizing Mie theory, but dust grains are decidedly not spherical. Mie theory can also be employed to calculate opacities of a population of dust grains with particular size or shape distributions (such as spheroids or ellipsoids), albeit with significant caveats (Bohren and Huffman, 1983; Min *et al.*, 2003). Some of these distributions provide decent approximations to the opacities of real powders or other distributions of particles.

Min *et al.* (2003) performed an extensive study of the shape effects in scattering and absorption by small particles. They found that all shape distributions other than homogeneous spheres matched the position of maxima from astronomical objects (circumstellar dust). A distribution of hollow spheres provided the overall best fit to the observations in the Min

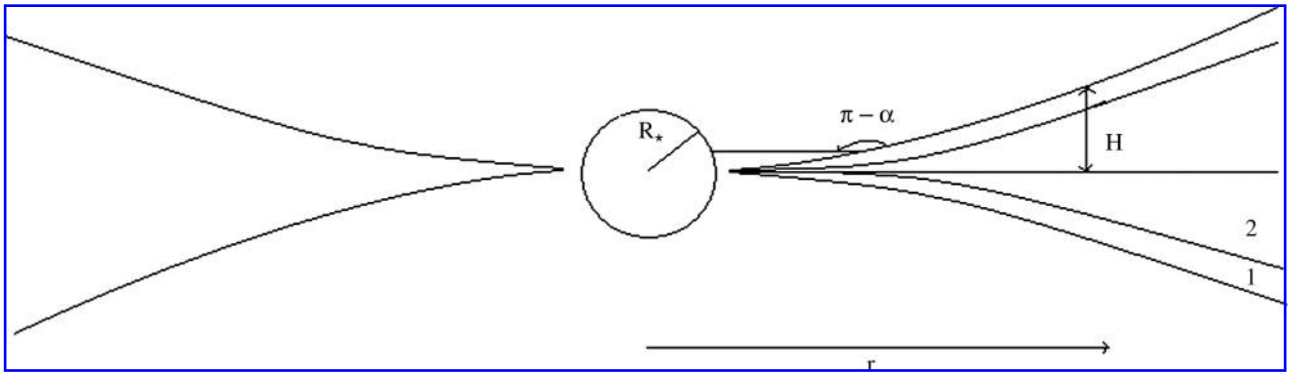

FIG. 2. Passive, reprocessing disk, where α is the grazing angle, *H* is the height of the visible photosphere, *r* is the distance from the star to the disk, area 1 is the superheated dust layer, and area 2 is the disk interior.

et al. (2003) study, which led to our decision to employ this shape distribution in the present study.

Protoplanetary disk model

The disk model presented in this study is based on the Chiang and Goldreich (1997) model of a passive, flared disk in hydrostatic and radiative equilibrium (Fig. 2). We consider only those cases in radiative equilibrium as well, where the radiation emitted from a particle of dust is equal to the radiation absorbed. In this study, however, we have calculated dust opacities, using a distribution of hollow spheres and a population of grains of different compositions, as opposed to the simple opacity approximation used by Chiang and Goldreich (1997). We also corrected an apparent error of a factor of $2^{1/4}$ in the equation for effective temperature given by Chiang and Goldreich (1997). In addition, Kurucz (1993) models of stellar atmospheres were used, rather than simply modeling the central star as a blackbody.

The parameters of our model include a T Tauri star of effective surface temperature, $T_* = 6000\,\mathrm{K}$; mass, $M_* = 1\,M_\odot$; and radius, $R_* = 1\,R_\odot$; with a passive, flared, reprocessing disk (face-on). The distance to the star was chosen to be 145 parsecs (approximately the distance to the Taurus-Auriga star-forming region). The inner radius of the disk is located 2 AU from the central star, and the outer radius of the disk was set at 80 AU. The model SED that resulted from these parameters is shown in Fig. 3.

Results

The composition of the dust and the relative percentages of each mineral used in our model are shown in Table 3. Opacities were calculated based upon a grain size of 0.1 μm, because we expect the dust in protoplanetary disks to exist in a quasi–steady-state size distribution, with the smallest particles being submicron in size (Weidenschilling, 2000; Dullemond and Dominik, 2005). The presence of submicron dust, even after many Myr of disk evolution, is strongly argued for; observations of the 10 μm silicate feature suggest that grains smaller than 2 μm in radius exist for several Myr in disks (van Boekel *et al.,* 2004; Dullemond and Dominik, 2005). Micron-sized dust also exists in the form of matrix grains in chondrites that formed many Myr after CAIs formed (Brearley, 1996). Additionally, although composite aggregates are expected in protoplanetary disks, it is customary to model them by assuming collections of smaller particles of various composition (van Boekel *et al.,* 2005; Min *et al.,* 2008). The effect of phyllosilicates on the spectra was tested by replacing 3% (as derived earlier; see *The disk environment*) of the amorphous forsterite with an equal amount of saponite (the most common phyllosilicate found in the matrix of meteorites).

TABLE 3. RELATIVE PERCENTAGES OF THE MINERALS USED IN MODELED SEDS

	Mineral without phyllosilicates	*Percentages with phyllosilicates*
Amorphous forsterite	58	55
Amorphous enstatite	32	32
Crystalline olivine	3	3
Crystalline enstatite	2	2
FeS (troilite)	2	2
Quartz	2	2
Hibonite	1	1
Saponite	0	3

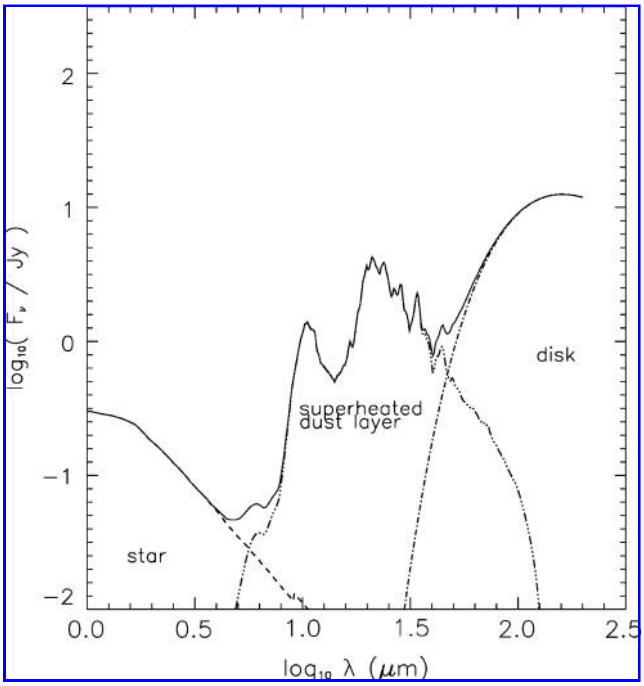

FIG. 3. Model SED of a passive, flared, radiative equilibrium disk, showing contributions from the star, the disk, and the superheated dust layer.

The difference in the SED that resulted from the inclusion of 3% phyllosilicates is certainly evident, as shown in Fig. 4. To ensure that the difference observed was due to the inclusion of phyllosilicates, rather than the decrease in the amount of amorphous forsterite, model SEDs were produced with 75% amorphous forsterite and 12% amorphous enstatite in one case and 12% amorphous forsterite and 75% amorphous enstatite in another (with all other relative percentages remaining the same as in Table 3). The difference between the SEDs with and without the inclusion of 3% phyllosilicates was still evident.

Inspection of Fig. 4 shows that the overall flux is increased with the inclusion of phyllosilicates, with the major spectral features located at the same wavelength as without phyllosilicates. At first glance, it would seem that it would be difficult to distinguish between an SED with or without phyllosilicates. While there are measurable differences in the calculated models with and without phyllosilicates, broad differences in level can be difficult to detect in the spectra of astrophysical objects due to uncertainties in the exact shape of the underlying continuum and foreground extinction and screening, as well as the difficulty of doing absolute spectrophotometry. The sensitivities of instruments in the infrared are rarely known better than a few percent because of the difficulty of calibration and the fact that they do not count photons. In practical settings, detection is both easier and more reliable if it involves comparison of distinct features that can be isolated from the background.

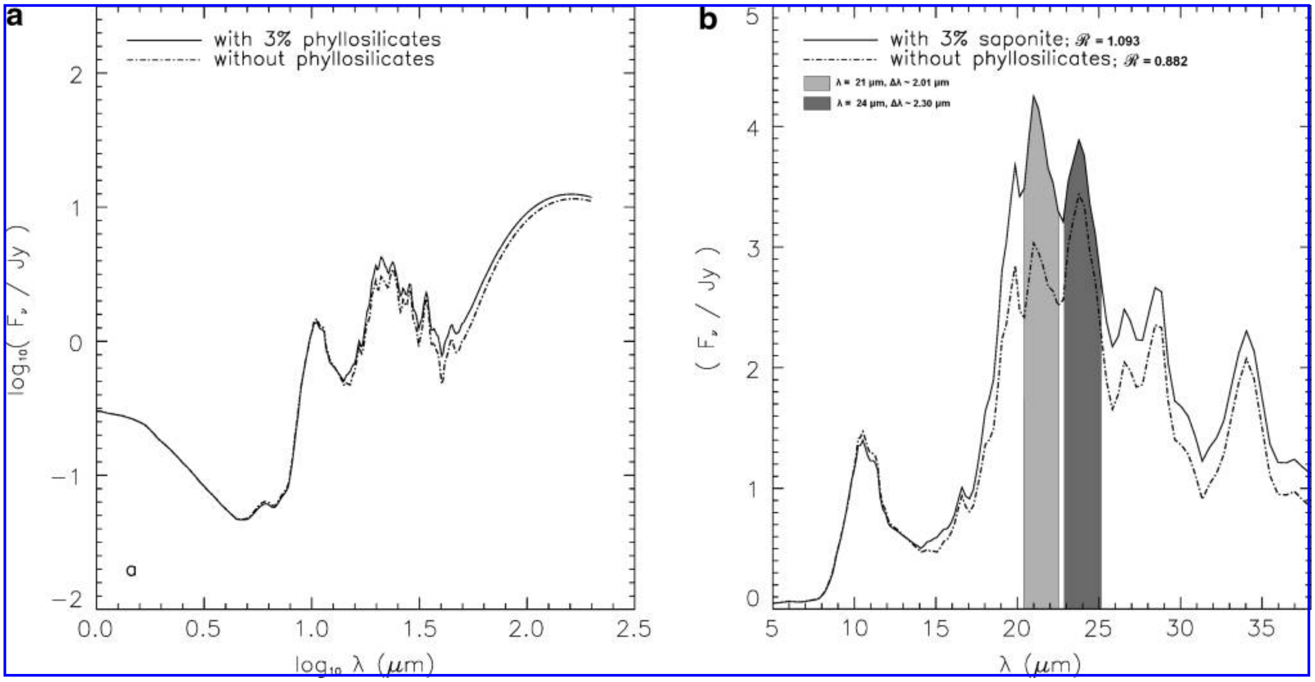

FIG. 4. (**a**) Model SED with and without the inclusion of 3% phyllosilicates. (**b**) Close-up view of the area of the SED where the contribution from the superheated dust layer dominates.

Upon closer examination of the model SED shown in Fig. 4, one can see higher emission at $\sim 21\,\mu$m than $\sim 24\,\mu$m in the SED including phyllosilicates. In the SED without phyllosilicates, however, the reverse is true; the $\sim 24\,\mu$m emission is stronger than the $\sim 21\,\mu$m emission. The ratio of these two features allows one to approach the question of detectability quantitatively. As the model SED shown in Fig. 4 is representative of the inclusion of saponite, we first sought to determine whether the same trend is seen when including different species of phyllosilicates. Model SEDs with the inclusion of 3% serpentine, montmorillonite, or cronstedtite are shown in Fig. 5. For the model SED with the inclusion of saponite, the flux ratio is $F_{21}/F_{24} = 1.093$, as opposed to the model SED without the inclusion of phyllosilicates, $F_{21}/F_{24} = 0.882$. The model SEDs with the inclusion of serpentine, montmorillonite, and cronstedtite show $F_{21}/F_{24} = 1.065$, $F_{21}/F_{24} = 1.282$, and $F_{21}/F_{24} = 0.872$, respectively. It appears that the flux ratio, F_{21}/F_{24}, may be diagnostic of the presence of saponite, serpentine, and montmorillonite, though it is not diagnostic of the presence of cronstedtite. Figure 6 shows a "color-color" plot of the model SEDs.

Possibility for detection

The question remains as to whether the detection of the effects of phyllosilicates on the $21/24\,\mu$m ratio is possible with the instruments available (or soon to be available). In the model SED that includes saponite, the flux at $21\,\mu$m is ~ 4250 mJy, and the flux at $24\,\mu$m is ~ 3889 mJy. This is well above the sensitivities for the instruments under consideration (see Table 4). Based upon the model SED (with the inclusion of saponite, $R = 10.4$, $F_{\lambda_1} = 4250$ mJy, and $F_{\lambda_2} = 3889$ mJy), we determined the minimum instrument-specific integration time, t, necessary to achieve a 1σ detection of $\Re = F_{\lambda_1}/F_{\lambda_2}$, (see Appendix A):

$$t = \left(\frac{\Sigma_\Re}{\Sigma_0}\right)^2 \left(\frac{F_0}{\sqrt{F_{\lambda_1} F_{\lambda_2}}}\right) \left(\frac{R}{R_0}\right) t_0 \quad (1)$$

Table 4 shows t for the Spitzer Space Telescope, the Stratospheric Observatory for Infrared Astronomy (SOFIA), Michelle (Gemini North), the NASA Infrared Telescope, and the James Webb Space Telescope. The question remains as to whether the calculated minimum integration time is reasonable.

The minimum integration times for the Spitzer Space Telescope, SOFIA, and the James Webb Space Telescope indicate that it is possible to achieve a 1σ detection. For Michelle (Gemini North), the minimum integration time of $\sim 10^3$ s may be reasonable; however, background noise and dark current will become significant over that integration time. A closer examination of the noise contributions would be necessary to determine definitively whether it is possible to achieve a 1σ detection. A more careful analysis of the noise is also necessary for the NASA Infrared Telescope, as background and dark current may become problematic with an integration time of 10 min. The demonstration that phyllosilicates can be detected with the Spitzer Space Telescope is of particular value, considering the availability of large amounts of archived data on protoplanetary disks as a part of the Spitzer Legacy Science Program.

Discussion

The implications of detection of phyllosilicates within protoplanetary disks are immense. Since phyllosilicates are formed by the interaction of liquid water with rock on planetesimals, their presence would strongly point to the existence of liquid water on rocky bodies in such protoplanetary disks. Detection of phyllosilicates would represent the first, albeit indirect, discovery of liquid water in another planetary system. The presence of liquid water has obvious astrobiological implications, both for the commonality of systems like our own and the development of life elsewhere. Additionally, their abundance in the dust of the protoplanetary disk would verify numerical models (*e.g.,* Weidenschilling, 2000) that suggest strong recycling of material between the dust of the disk and the planetesimals in the disk.

If phyllosilicates can indeed be reliably detected in protoplanetary disks, sufficient statistics may be accumulated to probe the abundances of the short-lived radionuclide ^{26}Al in other planetary systems. The water worlds hypothesis put forth by Desch and Leshin (2004) first proposed that water content in terrestrial planets forming in a solar system is linked to the ^{26}Al abundance in that system, the star-forming environment in which that system formed, and observational signatures such as phyllosilicate emission. A prediction of the water worlds hypothesis is that disks in the Taurus-Auriga molecular cloud, which have not been exposed to supernova ejecta and therefore should contain low ^{26}Al ($^{26}\text{Al}/^{27}\text{Al} \ll 5\times10^{-7}$), will not exhibit phyllosilicate emission, but they would also be predicted to have water-rich terrestrial planets. On the other hand, disks in systems that were contaminated by supernova material, such as those in the Orion Ic and Id associations (Cunha and Lambert, 1992, 1994; Cunha *et al.,* 1998), likely (though not necessarily) will contain abundant ^{26}Al and produce planetesimals containing phyllosilicates and would be predicted to have water-poor planets, akin to Earth.

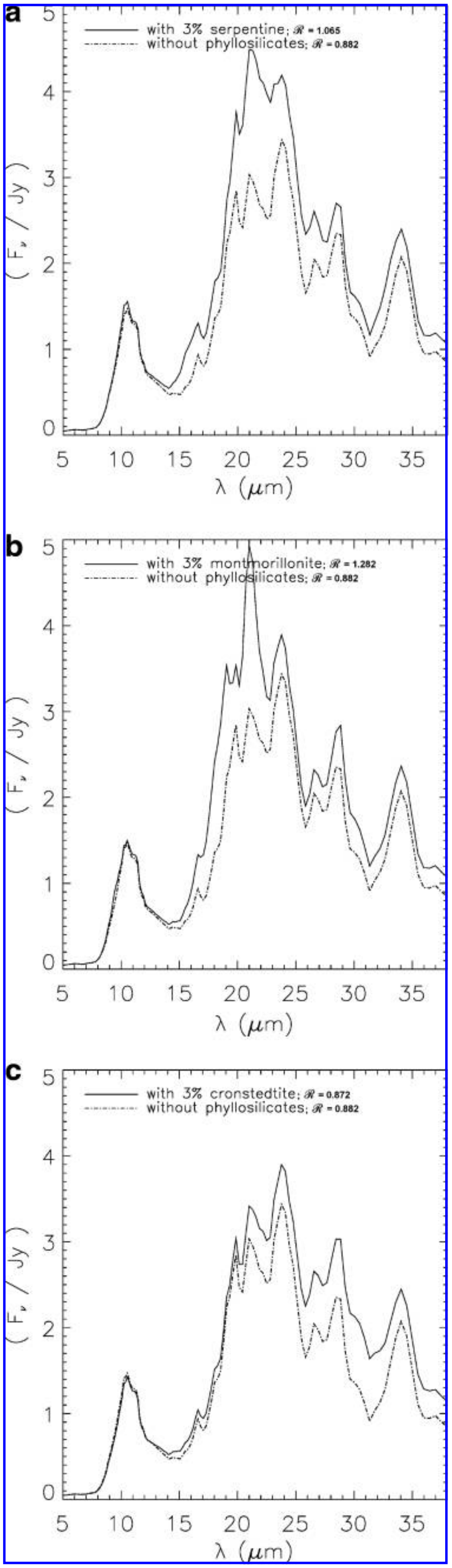

FIG. 5. Difference between the modeled spectrum with and without 3% (**a**) serpentine, (**b**) montmorillonite, or (**c**) cronstedtite.

Future work

In addition to phyllosilicates, carbonates are also important products of aqueous alteration (Mottl *et al.,* 2007). In addition to their presence in meteorites, Lisse *et al.* (2006) also tentatively identified the carbonates magnesite ($MgCO_3$) and siderite ($FeCO_3$) as components of the spectrum of the Deep Impact ejecta. Carbonates have strong emission features between 6 and 7 μm, outside of the 10 μm silicate emission band (Lane and Christensen, 1997). This lack of interference from silicates may enable the easy detection of carbonates. Future modeling will investigate this possibility by producing model SEDs with and without the inclusion of carbonates.

In the future, it would be worthwhile to investigate the spectral features and detectability of phyllosilicates that are less abundant. Lisse *et al.* (2006) tentatively identified nontronite in the spectra of comet 9P/Tempel 1. It would be appropriate to consider this and other phyllosilicates. For comparison with upcoming Herschel observations, it would also be highly appropriate to measure opacities at long wavelengths, out to 100 microns.

More sophisticated methods exist to model the absorption of radiation by particles; these methods have been shown to account for shape effects better than standard Mie theory. These include coupled dipole approximation and discrete dipole approximation. These other methods need to be utilized to produce model SEDs, with and without phyllosilicates, to compare to our results reported here.

Conclusion

In summary, phyllosilicates in the dust of protoplanetary disks impart an observable signature, especially in the 21–24 micron region. Fitting of model SEDs to disks observed by

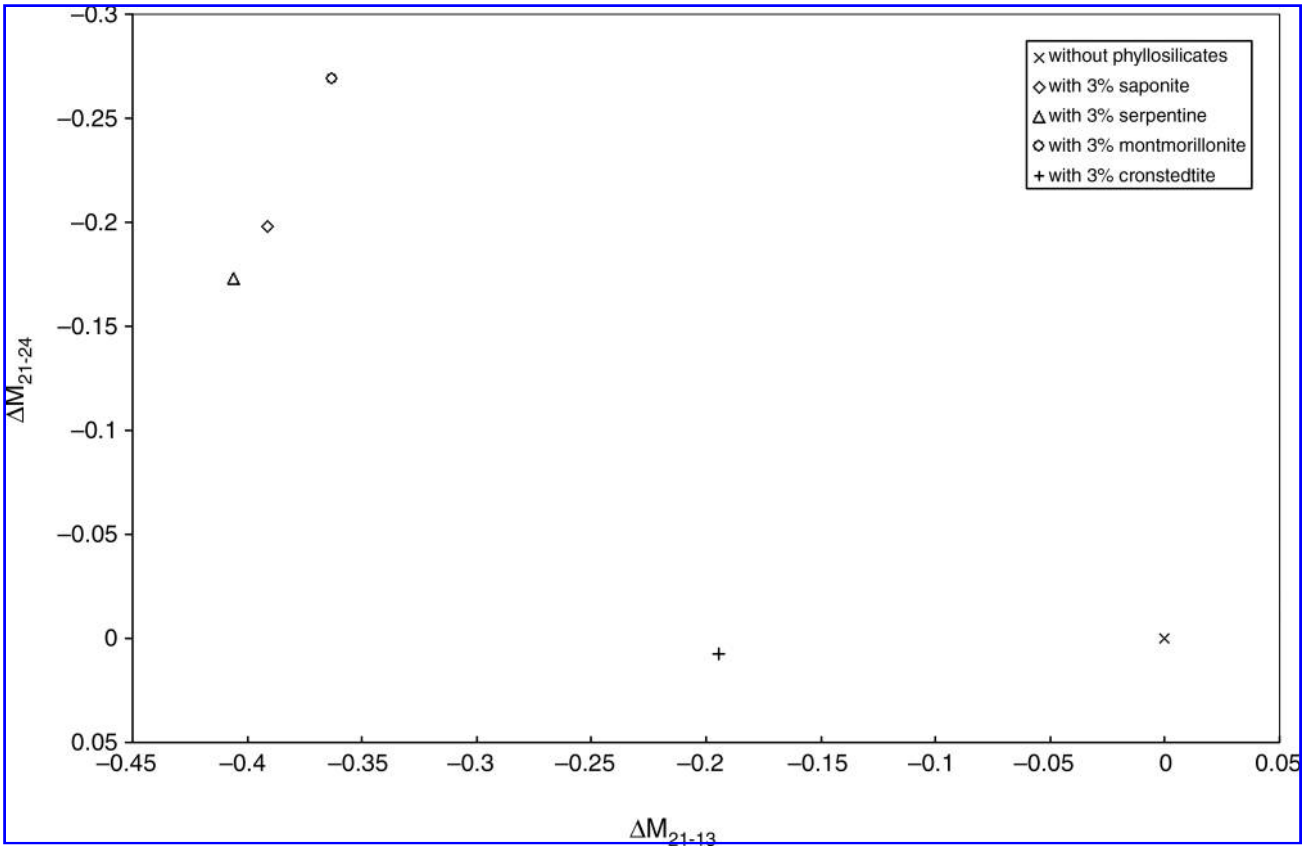

FIG. 6. "Color-color" diagram of the model fluxes, both with and without the addition of phyllosilicates. $\Delta M_{21-24} = -2.5\log_{10}(F_{21}/F_{24})$ and $\Delta M_{21-13} = -2.5\log_{10}(F_{21}/F_{13})$. The addition of phyllosilicates increases the F_{21}/F_{24} ratio (except in the case of cronstedtite) in approximately the same proportion that the F_{21}/F_{13} ratio increases. One can infer from this plot that phyllosilicates will show an increased flux at 21 μm.

infrared observatories, including the Spitzer Space Telescope, could resolve whether phyllosilicates are present at the few percent level. We expect phyllosilicates to be present in disks at levels such as these if formation and collisional destruction is rapid compared to disk evolution timescales, as predicted by numerical models, and if those planetesimals contain liquid water. The detection of phyllosilicates by the means outlined here would represent the first, albeit indirect, detection of liquid water on rocky bodies in planetary systems.

Appendix A

The noise present in the measured flux, F_λ, without the inclusion of phyllosilicates is given by

$$\sigma_{F_\lambda}^2 = Nt(I + S + D) + N\sigma_R^2 \qquad \text{(A1)}$$

where N is the number of pixels on which the signal is recorded, I is the intensity of the signal (in electrons/pixel) at a given wavelength, S is the background noise from the sky

Table 4. Minimum Integration Times Necessary for Detection of $\Re$

Telescope	*Instrument*	R[1]	*Sensitivity*[2]	t[3]
Spitzer	IRS	600	0.4 mJy	21.8 s
SOFIA	EXES	3000	2.7 Jy	59.8 s
Gemini North	Michelle	110	14 mJy	920.9 s
IRTF	MIRSI	100	100 mJy	383.8 s
JWST	MIRI	3000	5×10^{-20} Wm^{-2}	8.3×10^{-5} s

IRTF, the NASA Infrared Telescope; JWST, the James Webb Space Telescope.

[1] Spectral resolution, $R = \lambda/\Delta\lambda$, is given at the relevant wavelengths (21 and 24 μm).

[2] Sensitivities listed for IRS, EXES, Michelle, MIRSI, and MIRI are 1σ for an integration time of 512 s, 4σ for an integration time of 900 s, 5σ for an integration time of 1 hour, 1σ for an integration time of 60 s, and 10σ for an integration time of 10,000 s.

[3] Minimum integration times necessary to achieve a 1σ detection of $\Re$.

(in electrons/pixel/second; the conversion from the brightness, in ergs cm^{-2} s^{-1} μm^{-1}, involves the aperture and sensitivity of the instrument used to measure the signal), D is the dark current, t is the integration time, and σ_R is the read noise. The noise in the flux measured after the inclusion of phyllosilicates is

$$\sigma^2_{F_\lambda+\Delta F_\lambda} = Nt[(I+I\delta)+S+D]+N\sigma_R^2 \tag{A2a}$$

where $\delta = \Delta F_\lambda / F_\lambda$. Recalling that noise adds in quadrature, this gives the total noise in the difference as

$$\sigma^2_{\Delta F_\lambda} = \sigma^2_{F_\lambda} + \sigma^2_{F_\lambda+\Delta F_\lambda} = 2Nt(I+S+D)+NI\delta t+2N\sigma_R^2 \tag{A2b}$$

Absorbing the dark current into the background noise, the wavelength-dependent signal-to-noise in the difference, Σ_Δ, is then given by

$$\Sigma_\Delta = \frac{N(I\delta)t}{\sqrt{N}[2(I+S)t+2\sigma_R^2+\delta It]^{1/2}} \tag{A3}$$

Detectability thresholds for instruments are given in terms of the time, t_0 needed to detect a signal of strength I_0 with signal-to-noise, Σ_0.

$$\Sigma_0 = \frac{N_0 I_0 t_0}{\sqrt{N_0}[I_0 t_0 + S_0 t_0 + \sigma_R^2]^{1/2}} \tag{A4}$$

It is now possible to calculate what integration time is necessary to achieve the threshold signal-to-noise, Σ_0, of a number of instruments.

The spectral resolution, $R = \lambda/\Delta\lambda$, required for detection of the features at $\sim$21 and $\sim$24 μm, is determined by measuring the full width at half maximum of the feature at the given wavelength. R_0 is the spectral resolution reported on each instrument. The number of pixels over which the signal is recorded (the dispersion) must also be taken into account when determining spectral resolution. This results in the relationship $N/N_0 = R_0/R$, where $N = \Delta\lambda_R$/pixels, $N_0 = \Delta\lambda_{R_0}$/pixels. Using this relationship gives $N = N_0(R_0/R)$. As $I/I_0 = F_\lambda/F_0$, $I = (F_\lambda/F_0)I_0$, where F_0 is the flux measured at the given wavelength by the instrument (the sensitivity). Recall that $\delta = \Delta F_\lambda/F_\lambda$, which tells us $\Sigma_\Delta \propto \Delta F_\lambda/\sqrt{2F_\lambda}$. Assuming that $\sqrt{I} \gg \sigma_R^2$ (shot-noise limited), $\delta \ll 1$ (the difference in emission due to phyllosilicates is small compared to the total emission without phyllosilicates), the source is bright compared to the background ($S \ll I_0$), and the dark current is negligible ($D \ll I_0$) gives

$$\Sigma_\Delta = \frac{\Delta F_\lambda}{2F_\lambda F_0}\left(\frac{R_0}{R}\right)^{1/2}\left(\frac{t}{t_0}\right)^{1/2}\Sigma_0 \tag{A5}$$

For a 1σ detection of the ratio, $\Re = F_{\lambda_1}/F_{\lambda_2}$

$$\left(\frac{R_0}{R}\right)^{1/2}\left(\frac{t}{t_0}\right)^{1/2}\left(\frac{\sqrt{F_{\lambda_1}F_{\lambda_2}}}{F_0}\right)^{1/2}\Sigma_0 \geq \Sigma_\Re \tag{A6}$$

where $\Sigma_\Re$ is the signal-to-noise in the ratio. Solving for t gives the minimum instrument-specific integration time necessary to achieve a 1σ detection of $\Re$:

$$t = \left(\frac{\Sigma_\Re}{\Sigma_0}\right)^2\left(\frac{F_0}{\sqrt{F_{\lambda_1}F_{\lambda_2}}}\right)\left(\frac{R}{R_0}\right)t_0 \tag{A7}$$

Acknowledgments

Optical constants for amorphous forsterite and enstatite, and crystalline enstatite were taken from Jäger *et al.* (2003). Optical constants for crystalline olivine were taken from Fabian *et al.* (2001). Optical constants for troilite, quartz, and hibonite were taken from Begemann *et al.* (1994), Henning and Mutschke (1997), and Mutschke *et al.* (2002), respectively. Optical constants for the phyllosilicates (saponite, serpentine, montmorillonite, and cronstedtite) were obtained by Timothy Glotch (Glotch, 2006, personal communication; Glotch *et al.*, 2007).

This work was supported by NASA Origins of Solar Systems grant NNG06GI65G. We heartily thank Jeff Hester and Rolf Jansen for assistance on the observational aspects of the problem.

Author Disclosure Statement

No competing financial interests exist.

Abbreviations

AU, astronomical units; CAIs, calcium-rich, aluminum-rich inclusions; MIR, mid-infrared; SEDs, spectral energy distributions; SOFIA, Stratospheric Observatory for Infrared Astronomy; YSOs, young stellar objects.

References

Adams, F.C., Lada, C.J., and Shu, F.H. (1987) Spectral evolution of young stellar objects. *Astrophys. J.* 312:788–806.

Adams, F.C., Shu, F.H., and Lada, C.J. (1988) The disks of T Tauri stars with flat infrared spectra. *Astrophys. J.* 326:865–883.

Begemann, B., Dorschner, J., Henning, T., Mutschke, H., and Thamm, E. (1994) A laboratory approach to the interstellar sulfide dust problem. *Astrophys. J.* 423:L71–L74.

Beaulieu, J.P., Carey, S., Ribas, I., and Tinetti, G. (2008) Primary transit of the planet HD 189733b at 3.6 and 5.8 μm. *Astrophys. J.* 677:1343–1347.

Bockelee-Morvan, D., Gautier, D., Lis, D.C., Young, K., Keene, J., Phillips, T., Owen, T., Crovisier, J., Goldsmith, P.F., Bergin, E.A., Despois, D., and Wootten, A. (1998) Deuterated water in comet C/1996 B2 (Hyakutake) and its implications for the origin of comets. *Icarus* 133:147–162.

Bohren, C.F. and Huffman, D.R. (1983) *Absorption and Scattering of Light by Small Particles,* John Wiley & Sons, New York.

Boss, A.P. and Vanhala, H.A.T. (2000) Triggering protostellar collapse, injection, and disk formation. *Space Sci. Rev.* 92:13–22.

Bottke, W.F., Durda, D.D., Nesvorny, D., Jedicke, R., Morbidelli, A., Vokrouhlicky, D., and Levison, H.F. (2005) Linking the collisional history of the main asteroid belt to its dynamical excitation and depletion. *Icarus* 179:63–94.

Brauer, F., Dullemond, C.P., and Henning, T. (2008) Coagulation, fragmentation and radial motion of solid particles in protoplanetary disks. *Astron. Astrophys.* 480:859–877.

Brearley, A.J. (1996) Grain size distributions and textures in the matrices of metamorphosed CO3 chondrites [abstract 1080]. In *27th Lunar and Planetary Science Conference Abstracts,* Lunar and Planetary Institute, Houston.

Brownlee, D., Tsou, P., Aléon, J., Alexander, C.M.O.'D., Araki, T., Bajt, S., Baratta, G.A., Bastien, R., Bland, P., Bleuet, P., Borg, J., Bradley, J.P., Brearley, A., Brenker, F., Brennan, S., Bridges, J.C., Browning, N.D., Brucato, J.R., Bullock, E., Burchell, M.J., Busemann, H., Butterworth, A., Chaussidon, M., Cheuvront, A., Chi, M., Cintala, M.J., Clark, B.C., Clemett, S.J., Cody, G., Colangeli, L., Cooper, G., Cordier, P., Daghlian, C., Dai, Z., D'Hendecourt, L., Djouadi, Z., Dominguez, G., Duxbury, T., Dworkin, J.P., Ebel, D.S., Economou, T.E., Fakra, S., Fairey, S.A.J., Fallon, S., Ferrini, G., Ferroir, T., Fleckenstein, H., Floss, C., Flynn, G., Franchi, I.A., Fries, M., Gainsforth, Z., Gallien, J.-P., Genge, M., Gilles, M.K., Gillet, P., Gilmour, J., Glavin, D.P., Gounelle, M., Grady, M.M., Graham, G.A., Grant, P.G., Green, S.F., Grossemy, F., Grossman, L., Grossman, J.N., Guan, Y., Hagiya, K., Harvey, R., Heck, P., Herzog, G.F., Hoppe, P., Hörz, F., Huth, J., Hutcheon, I.D., Ignatyev, K., Ishii, H., Ito, M., Jacob, D., Jacobsen, C., Jacobsen, S., Jones, S., Joswiak, D., Jurewicz, A., Kearsley, A.T., Keller, L.P., Khodja, H., Kilcoyne, A.L.D., Kissel, J., Krot, A., Langenhorst, F., Lanzirotti, A., Le, L., Leshin, L.A., Leitner, J., Lemelle, L., Leroux, H., Liu, M.-C., Luening, K., Lyon, I., MacPherson, G., Marcus, M.A., Marhas, K., Marty, B., Matrajt, G., McKeegan, K., Meibom, A., Mennella, V., Messenger, K., Messenger, S., Mikouchi, T., Mostefaoui, S., Nakamura, T., Nakano, T., Newville, M., Nittler, L.R., Ohnishi, I., Ohsumi, K., Okudaira, K., Papanastassiou, D.A., Palma, R., Palumbo, M.E., Pepin, R.O., Perkins, D., Perronnet, M., Pianetta, P., Rao, W., Rietmeijer, F.J.M., Robert, F., Rost, D., Rotundi, A., Ryan, R., Sandford, S.A., Schwandt, C.S., See, T.H., Schlutter, D., Sheffield-Parker, J., Simionovici, A., Simon, S., Sitnitsky, I., Snead, C.J., Spencer, M.K., Stadermann, F.J., Steele, A., Stephan, T., Stroud, R., Susini, J., Sutton, S.R., Suzuki, Y., Taheri, M., Taylor, S., Teslich, N., Tomeoka, K., Tomioka, N., Toppani, A., Trigo-Rodríguez, J.M., Troadec, D., Tsuchiyama, A., Tuzzolino, A.J., Tyliszczak, T., Uesugi, K., Velbel, M., Vellenga, J., Vicenzi, E., Vincze, L., Warren, J., Weber, I., Weisberg, M., Westphal, A.J., Wirick, S., Wooden, D., Wopenka, B., Wozniakiewicz, P., Wright, I., Yabuta, H., Yano, H., Young, E.D., Zare, R.N., Zega, T., Ziegler, K., Zimmerman, L., Zinner, E., and Zolensky, M. (2006) Comet 81P/Wild 2 under a microscope. *Science* 314:1711–1716.

Buseck, P.R. and Hua, X. (1993) Matrices of carbonaceous chondrite meteorites. *Annu. Rev. Earth Planet. Sci.* 21:255–305.

Calvet, N., D'Alessio, P., Hartmann, L., Wilner, D., Walsh, A., and Sitko, M. (2002) Evidence for a developing gap in a 10 Myr old protoplanetary disk. *Astrophys. J.* 568:1008–1016.

Cameron, A.G.W. and Truran, J.W. (1977) The supernova trigger for formation of the Solar System. *Icarus* 30:447–461.

Carr, J.S. and Najita, J.R. (2008) Organic molecules and water in the planet formation region of young circumstellar disks. *Science* 319:1504–1506.

Chiang, E.I. and Goldreich, P. (1997) Spectral energy distributions of T Tauri stars with passive circumstellar disks. *Astrophys. J.* 490:368–376.

Chyba, C.F., Whitmire, D.P., and Reynolds, R. (2000) Planetary habitability and the origins of life. In *Protostars and Planets IV,* edited by V. Mannings, A.P. Boss, and S.S. Russell, The University of Arizona Press, Tucson, AZ, pp 1365–1393.

Ciesla, F.J., Lauretta, D.S., Cohen, B.A., and Hood, L.L. (2003) a nebular origin for chondritic fine-grained phyllosilicates. *Science* 299:549–552.

Cohen, B.A. and Coker, R.F. (2000) Modeling of liquid water on CM meteorite parent bodies and implications for amino acid racemization. *Icarus* 145:369–381.

Cunha, K. and Lambert, D.L. (1992) Chemical evolution of the Orion association. I—The oxygen abundance of main-sequence B stars. *Astrophys. J.* 399:586–598.

Cunha, K. and Lambert, D.L. (1994) Chemical evolution of the Orion association. 2: The carbon, nitrogen, oxygen, silicon, and iron abundances of main-sequence B stars. *Astrophys. J.* 426:170–191.

Cunha, K., Smith, V.V., and Lambert, D.L. (1998) Chemical evolution of the Orion association. IV. The oxygen and iron abundances of F and G stars. *Astrophys. J.* 493:195–205.

de Pater, I. and Lissauer, J.J. (2001) *Planetary Sciences,* Cambridge University Press, Cambridge, UK.

Desch, S.J. and Leshin, L.A. (2004) Making water worlds: the role of Al 26 [abstract 1987]. In *35th Lunar and Planetary Science Conference Abstracts,* Lunar and Planetary Institute, Houston.

Dorschner, J., Begemann, B., Henning, T., Jaeger, C., and Mutschke, H. (1995) Steps toward interstellar silicate mineralogy. II. Study of Mg-Fe-silicate glasses of variable composition. *Astron. Astrophys.* 300:503–520.

Drake, M.J. (1979) Geochemical evolution of the eucrite parent body—possible nature and evolution of asteroid 4 Vesta. In *Asteroids,* edited by T. Gehrels, The University of Arizona Press, Tucson, AZ, pp 765–782.

Drake, M.J. and Righter, K. (2002) Determining the composition of the Earth. *Nature* 416:39–44.

Dullemond, C.P. and Dominik, C. (2005) Dust coagulation in protoplanetary disks: a rapid depletion of small grains. *Astron. Astrophys.* 434:971–986.

Eberhardt, P., Reber, M., Krankowsky, D., and Hodges, R.R. (1995) The D/H and $^{18}O/^{16}O$ ratios in water from comet P/Halley. *Astron. Astrophys.* 302:301–316.

Fabian, D., Henning, T., Jäger, C., Mutschke, H., Dorschner, J., and Wehrhan, O. (2001) Steps toward interstellar silicate mineralogy. VI. Dependence of crystalline olivine IR spectra on iron content and particle shape. *Astron. Astrophys.* 378: 228–238.

Gail, H.-P. (1998) Chemical reactions in protoplanetary accretion disks. IV. Multicomponent dust mixture. *Astron. Astrophys.* 332:1099–1122.

Gail, H.-P. (2003) Formation and evolution of minerals in accretion disks and stellar outflows. In *Astromineralogy,* Lecture Notes in Physics, Vol. 609, Springer, Berlin-Heidelberg, pp 55–120.

Gail, H.-P. (2004) Radial mixing in protoplanetary accretion disks. IV. Metamorphosis of the silicate dust complex. *Astron. Astrophys.* 413:571–591.

Gilmour, J.D. and Middleton, C.A. (2009) Anthropic selection of a solar system with a high 26Al/27Al ratio: implications and a possible mechanism. *Icarus* 201:821–823.

Glotch, T.D., Rossman, G.R., and Aharonson, O. (2007) Mid-infrared (5–100 μm) reflectance spectra and optical constants of ten phyllosilicate minerals. *Icarus* 192:605–622.

Gradie, J. and Tedesco, E. (1982) Compositional structure of the asteroid belt. *Science* 216:1405–1407.

Grimm, R.E. and McSween, H.Y. (1993) Heliocentric zoning of the asteroid belt by aluminum-26 heating. *Science* 259:653–655.

Haisch, K.E., Jr., Lada, E.A., and Lada, C.J. (2001) Disk frequencies and lifetimes in young clusters. *Astrophys. J.* 553:L153–L156.

Hartmann, L. (1998) *Accretion Processes in Star Formation,* Cambridge University Press, Cambridge, UK.

Henning, T. and Mutschke, H. (1997) Low-temperature infrared properties of cosmic dust analogues. *Astron. Astrophys.* 327:743–754.

Hester, J.J., Desch, S.J., Healy, K.R., and Leshin, L.A. (2004) The cradle of the Solar System. *Science* 304:1116–1117.

Huss, G.R., MacPherson, G.J., Wasserburg, G.J., Russell, S.S., and Srinivasan, G. (2001) 26Al in CAIs and chondrules from unequilibrated ordinary chondrites. *Meteorit. Planet. Sci.* 36:975–997.

Jacobsen, S.B. (2005) The birth of the Solar System in a molecular cloud: evidence from the isotopic pattern of short-lived nuclides in the early Solar System. *Chondrites and the Protoplanetary Disk* 341:548–557.

Jäger, C., Dorschner, J., Mutschke, H., Posch, T., and Henning, T. (2003) Steps toward interstellar silicate mineralogy. VII. Spectral properties and crystallization behaviour of magnesium silicates produced by the sol-gel method. *Astron. Astrophys.* 408:193–204.

Johansen, A., Brauer, F., Dullemond, C., Klahr, H., and Henning, T. (2008) A coagulation-fragmentation model for the turbulent growth and destruction of preplanetesimals. *Astron. Astrophys.* 486:597–611.

Kalas, P., Liu, M.C., and Matthews, B.C. (2004) Discovery of a large dust disk around the nearby star AU Microscopii. *Science* 303:1990–1992.

Kemper, F., Vriend, W.J., and Tielens, A.G.G.M. (2004) The absence of crystalline silicates in the diffuse interstellar medium. *Astrophys. J.* 609:826–837.

Kenyon, S.J. and Hartmann, L. (1987) Spectral energy distributions of T Tauri stars—disk flaring and limits on accretion. *Astrophys. J.* 323:714–733.

Kojima, T. and Tomeoka, K. (1996) Indicators of aqueous alteration and thermal metamorphism on the CV parent body: microtextures of a dark inclusion from Allende. *Geochim. Cosmochim. Acta* 60:2651–2666.

Krishna Swamy, K.S. (2005) *Dust in the Universe. Similarities and Differences,* World Scientific Series in Astronomy and Astrophysics, Vol. 7, World Scientific Publishing, Singapore.

Krot, A.N., Scott, E.R., and Zolensky, M.E. (1995) Mineralogical and chemical modification of components in CV3 chondrites: nebular or asteroidal processing? *Meteoritics* 30: 748–775.

Krot, A.N., Hutcheon, I.D., Brearley, A.J., Pravdivtseva, O.V., Petaev, M.I., and Hohenberg, C.M. (2006) Timescales and settings for alteration of chondritic meteorites. In *Meteorites and the Early Solar System II,* edited by Dante S. Lauretta and Harry Y. McSween, The University of Arizona Press, Tucson, AZ, pp 525–553.

Kurucz, R.L. (1993) *Kurucz CD-ROM,* Smithsonian Astrophysical Observatory, Cambridge, MA.

Lane, M.D. and Christensen, P.R. (1997) Thermal infrared emission spectroscopy of anhydrous carbonates. *J. Geophys. Res.* 102:25581–25592.

Lauretta, D.S., Hua, X., and Buseck, P.R. (2000) Mineralogy of fine-grained rims in the ALH 81002 cm chondrite. *Geochim. Cosmochim. Acta* 64:3263–3273.

Lee, T., Papanastassiou, D.A., and Wasserburg, G.J. (1976) Demonstration of Mg-26 excess in Allende and evidence for Al-26. *Geophys. Res. Lett.* 3:41–44.

Léger, A., Selsis, F., Sotin, C., Guillot, T., Despois, D., Mawet, D., Ollivier, M., Labèque, A., Valette, C., Brachet, F., Chazelas, B., and Lammer, H. (2004) A new family of planets? "Ocean-Planets." *Icarus* 169:499–504.

Levison, H.F., Dones, L., Chapman, C.R., Stern, S.A., Duncan, M.J., and Zahnle, K. (2001) Could the lunar "Late Heavy Bombardment" have been triggered by the formation of Uranus and Neptune? *Icarus* 151:286–306.

Lisse, C. (2002) On the role of dust mass loss in the evolution of comets and dusty disk systems. *Earth Moon Planets* 90:497–506.

Lisse, C.M., VanCleve, J., Adams, A.C., A'Hearn, M.F., Fernández, Y.R., Farnham, T.L., Armus, L., Grillmair, C.J., Ingalls, J., Belton, M.J.S., Groussin, O., McFadden, L.A., Meech, K.J., Schultz, P.H., Clark, B.C., Feaga, L.M., and Sunshine, J.M. (2006) Spitzer spectral observations of the Deep Impact ejecta. *Science* 313:635–640.

Looney, L.W., Tobin, J.J., and Fields, B.D. (2006) Radioactive probes of the supernova-contaminated solar nebula: evidence that the Sun was born in a cluster. *Astrophys. J.* 652:1755–1762.

Lugmair, G.W. and Shukolyukov, A. (2001) Early Solar System events and timescales. *Meteorit. Planet. Sci.* 36:1017–1026.

MacPherson, G.J., Davis, A.M., and Zinner, E.K. (1995) The distribution of aluminum-26 in the early Solar System—a reappraisal. *Meteoritics* 30:365–386.

McCaughrean, M.J. and O'Dell, C.R. (1996) Direct imaging of circumstellar disks in the Orion Nebula. *Astron. J.* 111:1977–1986.

McSween, H.Y., Jr., Ghosh, A., Grimm, R.E., Wilson, L., and Young, E.D. (2002) Thermal evolution models of asteroids. In *Asteroids III,* edited by W.F. Bottke, P. Paolicchi, R.P. Binzel, and A. Cellino, The University of Arizona Press, Tucson, AZ, pp 559–571.

Meier, R., Wellnitz, D., Kim, S.J., and A'Hearn, M.F. (1998) The NH and CH bands of comet C/1996 B2 (Hyakutake). *Icarus* 136:268–279.

Min, M., Hovenier, J.W., and de Koter, A. (2003) Shape effects in scattering and absorption by randomly oriented particles small compared to the wavelength. *Astron. Astrophys.* 404: 35–46.

Min, M., Hovenier, J.W., Waters, L.B.F.M., and de Koter, A. (2008) The infrared emission spectra of compositionally inhomogeneous aggregates composed of irregularly shaped constituents. *Astron. Astrophys.* 489:135–141.

Morbidelli, A., Chambers, J., Lunine, J.I., Petit, J.M., Robert, F., Valsecchi, G.B., and Cyr, K.E. (2000) Source regions and time scales for the delivery of water to Earth. *Meteorit. Planet. Sci.* 35:1309–1320.

Mottl, M.J., Glazer, B.T., Kaiser, R.I., and Meech, K.J. (2007) Water and astrobiology. *Chem. Erde* 67:253–282.

Mutschke, H., Posch, Th., Fabian, D., and Dorschner, J. (2002) Towards the identification of circumstellar hibonite. *Astron. Astrophys.* 392:1047–1052.

Nakamura, R. (1998) Optical properties of dust aggregates in the disk of Beta Pictoris. *Earth, Planets, and Space* 50:587–593.

Nesvorny, D., Vokrouhlicky, D., Bottke, W.F., and Sykes, M. (2006) Physical properties of asteroid dust bands and their sources. *Icarus* 181:107–144.

Okamoto, Y.K., Kataza, H., Honda, M., Yamashita, T., Onaka, T., Watanabe, J., Miyata, T., Sako, S., Fujiyoshi, T., and Sakon, I. (2004) An early extrasolar planetary system revealed by planetesimal belts in β Pictoris. *Nature* 431:660–663.

Ouellette, N., Desch, S.J., Hester, J.J., and Leshin, L.A. (2005) A nearby supernova injected short-lived radionuclides into our protoplanetary disk. *Chondrites and the Protoplanetary Disk* 341:527–538.

Ouellette, N., Desch, S.J., and Hester, J.J. (2007) Interaction of supernova ejecta with nearby protoplanetary disks. *Astrophys. J.* 662:1268–1281.

Owen, T. and Bar-Nun, A. (1995) Comets, impacts and atmospheres. *Icarus* 116:215–226.

Pollack, J.B., Hollenbach, D., Beckwith, S., Simonelli, D.P., Roush, T., and Fong, W. (1994) Composition and radiative properties of grains in molecular clouds and accretion disks. *Astrophys. J.* 421:615–639.

Raymond, S.N., Quinn, T., and Lunine, J.I. (2004) Making other earths: dynamical simulations of terrestrial planet formation and water delivery. *Icarus* 168:1–17.

Raymond, S.N., Quinn, T., and Lunine, J.I. (2006) High-resolution simulations of the final assembly of Earth-like planets I. Terrestrial accretion and dynamics. *Icarus* 183:265–282.

Reach, W.T., Morris, P., Boulanger, F., and Okumura, K. (2003) The mid-infrared spectrum of the zodiacal and exozodiacal light. *Icarus* 164:384–403.

Rubin, A.E. (1997) Mineralogy of meteorite groups. *Meteorit. Planet. Sci.* 32:231–247.

Selsis, F., Kasting, J.F., Levrard, B., Paillet, J., Ribas, I., and Delfosse, X. (2007) Habitable planets around the star Gliese 581? *Astron. Astrophys.* 476:1373–1387.

Smith, B.A. and Terrile, R.J. (1984) A circumstellar disk around Beta Pictoris. *Science* 226:1421–1424.

Srinivasan, G., Goswami, J.N., and Bhandari, N. (1999) 26Al in Eucrite Piplia Kalan: plausible heat source and formation chronology. *Science* 284:1348–1350.

Stephan, T. (2008) Assessing the elemental composition of comet 81P/Wild 2 by analyzing dust collected by Stardust. *Space Sci. Rev.* 138:247–258.

Swindle, T.D. and Kring, D.A. (1997) Implications of small comets for the noble gas inventories of Earth and Mars. *Geophys. Res. Lett.* 24:3113–3116.

Throop, H.B., Bally, J., Esposito, L.W., and McCaughrean, M.J. (2001) Evidence for dust grain growth in young circumstellar disks. *Science* 292:1686–1698.

Tomeoka, K. and Buseck, P.R. (1990) Phyllosilicates in the Mokoia CV carbonaceous chondrite—evidence for aqueous alteration in an oxidizing environment. *Geochim. Cosmochim. Acta* 54:1745–1754.

Udry, S., Bonfils, X., Delfosse, X., Forveille, T., Mayor, M., Perrier, C., Bouchy, F., Lovis, C., Pepe, F., Queloz, D., and Bertaux, J.L. (2007) The HARPS search for southern extra-solar planets. XI. Super-Earths (5 and 8 $M_\odot$) in a 3-planet system. *Astron. Astrophys.* 469:L43–L47.

van Boekel, R., Min, M., Leinert, Ch., Waters, L.B.F.M., Richichi, A., Chesneau, O., Dominik, C., Jaffe, W., Dutrey, A., Graser, U., Henning, Th., de Jong, J., Köhler, R., de Koter, A., Lopez, B., Malbet, F., Morel, S., Paresce, F., Perrin, G., Preibisch, Th., Przygodda, F., Schöller, M., and Wittkowski, M. (2004) The building blocks of planets within the "terrestrial" region of protoplanetary disks. *Nature* 432:479–482.

van Boekel, R., Min, M., Waters, L.B.F.M., de Koter, A., Dominik, C., van den Ancker, M.E., and Bouwman, J. (2005) A 10 μm spectroscopic survey of Herbig Ae star disks: grain growth and crystallization. *Astron. Astrophys.* 437:189–208.

van Schmus, W.R. and Wood, J.A. (1967) A chemical-petrologic classification for the chondritic meteorites. *Geochim. Cosmochim. Acta* 31:747.

Wadhwa, M. and Russell, S.S. (2000) Timescales of accretion and differentiation in the early Solar System: the meteoritic evidence. In *Protostars and Planets IV,* edited by V. Mannings, A.P. Boss, and S.S. Russell, The University of Arizona Press, Tucson, AZ, pp 995–1018.

Wadhwa, M., Amelin, Y., Davis, A.M., Lugmair, G.W., Meyer, B., Gounelle, M., and Desch, S.J. (2007) From dust to planetesimals: implications for the solar protoplanetary disk from short-lived radionuclides. In *Protostars and Planets V*, edited by B. Reipurth, D. Jewitt, and K. Keil, The University of Arizona Press, Tucson, AZ, pp 835–848.

Watson, D.M., Bohac, C.J., Hull, C., Forrest, W.J., Furlan, E., Najita, J., Calvet, N., D'Alessio, P., Hartmann, L., Sargent, B., Green, J.D., Kim, K.H., Kyoung, H., and Houck, J.R. (2007) The development of a protoplanetary disk from its natal envelope. *Nature* 448:1026–1028.

Weidenschilling, S.J. (1977) The distribution of mass in the planetary system and solar nebula. *Astrophys. Space Sci.* 51:153–158.

Weidenschilling, S.J. (2000) Formation of planetesimals and accretion of the terrestrial planets. *Space Sci. Rev.* 92:295–310.

Weidenschilling, S.J. and Cuzzi, J.N. (2006) Accretion dynamics and timescales: relation to chondrites. In *Meteorites and the Early Solar System II,* edited by D.S. Lauretta and H.Y. McSween, The University of Arizona Press, Tucson, AZ, pp 473–485.

Weidenschilling, S.J., Spaute, D., Davis, D.R., Marzari, F., and Ohtsuki, K. (1997) Accretional evolution of a planetesimal swarm. *Icarus* 128:429–455.

Weidenschilling, S.J., Davis, D.R., and Marzari, F. (2001) Very early collisional evolution in the asteroid belt. *Earth, Planets, and Space* 53:1093–1097.

Weisberg, M.K., McCoy, T.J., and Krot, A.N. (2006) Systematics and evaluation of meteorite classification. In *Meteorites and the Early Solar System II,* edited by D.S. Lauretta and H.Y. McSween, The University of Arizona Press, Tucson, AZ, pp 19–52.

Williams, D.M. and Gaidos, E. (2008) Detecting the glint of starlight on the oceans of distant planets. *Icarus* 195:927–937.

Wooden, D., Desch, S., Harker, D., Gail, H.P., and Keller, L. (2007) Comet grains and implications for heating and radial mixing in the protoplanetary disk. In *Protostars and Planets V,* edited by B. Reipurth, D. Jewitt, and K. Keil, The University of Arizona Press, Tucson, AZ, pp 815–833.

Woolum, D.S. and Cassen, P. (1999) Astronomical constraints on nebular temperatures: implications for planetesimal formation. *Meteorit. Planet. Sci.* 34:897–907.

Wyatt, S.P. and Whipple, F.L. (1950) The Poynting-Robertson effect on meteor orbits. *Astrophys. J.* 111:134–141.

Zolensky, M., Nakamura-Messenger, K., Rietmeijer, F., Leroux, H., Mikouchi, T., Ohsumi, K., Simon, S., Grossman, L., Stephan, T., Weisberg, M., Velbel, M., Zega, T., Stroud, R., Tomeoka, K., Ohnishi, I., Tomioka, N., Nakamura, T., Matrajt, G., Joswiak, D., Brownlee, D., Langenhorst, F., Krot, A., Kearsley, A., Ishii, H., Graham, G., Dai, Z.R., Chi, M., Bradley, J., Hagiya, K., Gounelle, M., and Bridges, J. (2008) Comparing Wild 2 particles to chondrites and IDPs. *Meteorit. Planet. Sci.* 43:261–272.

Zuckerman, B., Song, I., Bessell, M.S., and Webb, R.A. (2001) The β Pictoris moving group. *Astrophys. J.* 562:L87–L90.

Address correspondence to:
Melissa A. Morris
Department of Physics, Astronomy, and Materials Science
Missouri State University
901 S. National Ave.
Springfield, MO 65897

E-mail: melissamorris@missouristate.edu